INSTITUTE OF PHYSICS PUBLISHING SEMICONDUCTOR SCIENCE AND TECHNOLOGY

Semicond. Sci. Technol. **20** (2005) 80–85 doi:10.1088/0268-1242/20/1/013

Absorption and reflection analysis of transparent conductive Ga-doped ZnO films

N R Aghamalyan, E A Kafadaryan, R K Hovsepyan and S I Petrosyan

Institute for Physical Research NAS of Armenia, Ashtarak-2, 378410, Armenia

E-mail: natagam@ipr.sci.am

Received 1 June 2004, in final form 20 September 2004
Published 9 December 2004
Online at stacks.iop.org/SST/20/80

Abstract

Transparent conductive films of 2 at% Ga-doped ZnO films were prepared on C-plane sapphire substrates by e-beam evaporation in vacuum. The optical absorption, reflectance, structural and electrical properties of 2 at% Ga-doped ZnO films were investigated. The films are highly transparent (>80%) in visible–NIR ranges, and the optical bandgap exhibits a blue shift for the as-deposited films from 3.30 eV to 3.83 eV and for heat treatment from 3.27 eV to 3.60 eV for 2 at% Ga-doped ZnO films with respect to pure ZnO films. Through resistivity, optical constants (ε, σ, –Im ε^{-1} and ω_p) and carrier concentration obtained from reflectivity and transmittance spectra for 2 at% Ga-doped ZnO films, we found that these films behave as n-type semiconductors exhibiting high carrier concentration $N \sim 10^{21}$ cm^{-3}. This also gives an opportunity to predict electrical behaviour of transparent conductive films on the basis of the analysis of absorption and reflection measurements.

1. Introduction

Transparent conductive oxides (TCO) have a range of highly useful applications such as transparent electrodes in opto-electronic devices and solar cells. Most previous investigations on TCO films have focused on indium tin oxides (ITO) or tin oxides (SnO_2); however, recently ZnO films have been promoted as their alternatives with advantages of low cost, resource availability and nontoxicity.

Intrinsic ZnO is an n-type wide bandgap semiconductor with the hexagonal wurtzite structure. Stoichiometric nondoped ZnO films have high resistivity due to the low carrier density; however, usually ZnO films show n-type conduction due to oxygen deficiencies and interstitial Zn ions that act as donors in the ZnO lattice. The addition of impurities in wide bandgap semiconductors often induces dramatic changes in their electrical and optical properties. It is well known that group III elements such as Al, In and Ga act as donors in ZnO. The Ga-doped ZnO has been prepared using magnetron sputtering [1, 2], molecular beam epitaxy [3], pulsed laser deposition [4, 5], sol–gel [6, 7], chemical vapour deposition [8] and others.

In this paper, the influence of the gallium impurity on structural, optical and electrical properties of ZnO films prepared by e-beam evaporation is reported. Comparisons of the structural, electrical and optical properties of ZnO films before and after post-heat treatment are discussed. Optical and electrical characteristics, such as the refractive index, absorption and reflectivity as a function of photon energy and also the energy bandgap and electrical resistivity are analysed to see the effect of impurity and post-heat treatment on them.

2. Experimental procedure

Pure ZnO and Ga-doped ZnO were prepared by the e-beam deposition technique in vacuum [9] by using (0001) sapphire as the substrate. Sintered ceramic pellets of pure ZnO and 2 at% Ga-doped ZnO were used as targets. All the samples were prepared at the same deposition conditions: electron energy was ~6 keV, substrate temperature was maintained at 223 °C and film growth rate was 1.45 Å s^{-1}. After deposition, the films were heated at 350 °C for 1 h in air to improve crystallinity and optical quality. The ZnO films obtained at such conditions were absolutely transparent and had high mechanical hardness.

Table 1. Ga content, film thickness, d, lattice parameters, c, crystallite size, D, energy bandgap, E_g, empirical parameter, E_0 and electrical resistivity, ρ, of the as-deposited and annealed Ga-doped ZnO films.

Ga (at%)	d (nm)	c (Å)	FWHM (0002) (°)	D (nm)	E_g (eV)	E_0 (meV)	ρ (Ω cm)
2, as-deposited	365 ± 10	5.188	0.367	22	3.83	467	0.36×10^{-3}
2, annealed	400 ± 10	5.175	0.333	25	3.60	356	1.48×10^{-3}
0, as-deposited	870 ± 10	5.195	0.333	25	3.30	84	1×10^{-2}
0, annealed	870 ± 10	5.195	0.333	25	3.27	94	1.8×10^{-1}

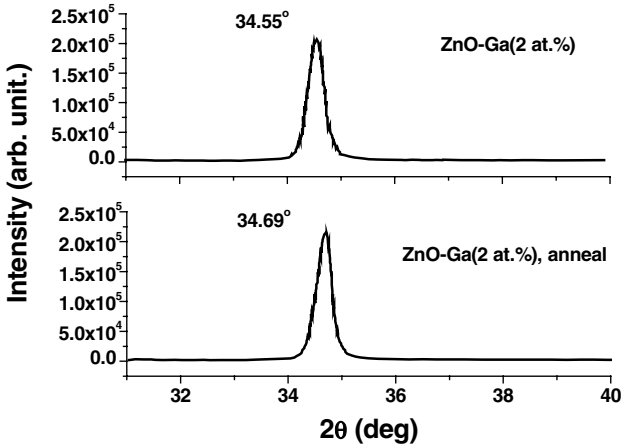

Figure 1. XRD spectra for both annealed and as-deposited 2 at% Ga-doped ZnO films.

The crystalline quality and orientation of 2 at% Ga-doped ZnO films were established by x-ray diffraction (XRD). The optical transmission and reflection spectra were recorded using ultraviolet–visible and infrared spectrophotometers at room temperature. Sheet resistance R was measured by the four-probe technique for 1 kHz frequency.

3. Results and discussion

3.1. Structural properties

In this work, e-beam evaporation in vacuum was used for producing high-quality ZnO films on sapphire substrates at low temperatures. The results of XRD analysis of the Ga-doped ZnO films deposited on (0001) sapphire showed that the Ga doping does not change the structure of ZnO, and the obtained films have a good crystalline structure with preferential orientation along the (0002) axis. In figure 1 XRD spectra of 2 at% Ga-doped ZnO films for both as-deposited and post-annealed samples are shown. It is seen that after annealing the (0002) peak is slightly narrowed. The crystallite sizes of the Ga-doped ZnO films were changed slightly from 22 to 25 nm. The XRD spectra obtained from the FWHM of the (0002) diffraction peak, the estimated values of lattice parameter c and crystallite size D calculated from the FWHM of the (0002) diffraction peak using Sherrer's formula [10] for the as-deposited and annealed Ga-doped ZnO films are summarized in table 1.

3.2. Electrical measurement

The conduction characteristics of pure ZnO are primarily dominated by electrons generated by the oxygen vacancies (V_O) and zinc interstitial atoms (Zn_i) [11]. Electrical resistivity of Ga-doped ZnO films is lower than that of pure ZnO films. The introduction of Ga can increase free electron density by substituting the host atoms (Zn) [12]. It is believed that Ga is able to ionize into Ga^{3+} and replace Zn^{2+}, so that it can contribute a free electron from each Ga atom. Accumulations of these electrons form electron gases that act as charge carriers and reduce resistance.

The measured sheet resistance (R) and the thickness of the films (d) were used to calculate the electrical resistivity (ρ) of the samples, using the expression $\rho = Rd$. The electrical resistivity ρ for pure and 2 at% Ga-doped films for the as-deposited and the heat-treated ZnO films are given in table 1. The electrical resistivity decreases from 0.18 Ω cm for pure ZnO films to 1.48×10^{-3} Ω cm for the 2 at% Ga in the case of heat-treated films and from 1×10^{-2} Ω cm to 0.36×10^{-3} Ω cm for the as-deposited films. It is also seen that the resistivity of the heat-treated films in air is higher compared to that of the as-deposited films. The resistivity increase by the heat treatment is mainly due to the decrease in carrier concentration.

3.3. Optical absorption measurements

The optical transmittance (T) of the films is plotted in figure 2 as a function of ω wavenumbers in the wavelength range 0.3–40 μm. The films exhibit more than 80% of transmittance in the visible wavelength region with some interference fringes and sharp ultraviolet absorption edges. The main differences are in the near-infrared range, where the transmittance decreases continuously and reflectance increases for the samples.

In the UV region, the optical transmittance of the film falls sharply due to the onset of the fundamental absorption in this region. The measured transmittance was converted into the absorption coefficient α, using the relationship $\alpha(\lambda) = 1/d \ln[(1-R)^2/T]$, where d is the film thickness, which was determined using interference fringes in optical spectra by the method proposed in [13]. The photon energy dependences of the absorption coefficient near UV edge of the Ga-doped ZnO films are shown in figure 3.

The energy gap (E_g) can be estimated by assuming a direct transition between valence and conduction bands. The absorption coefficient α as a function of photon energy $h\nu$ can be expressed as $(\alpha h\nu)^2 = A(h\nu - E_g)$, where A is a constant. The dependences $(\alpha h\nu)^2$ versus energy $h\nu$ for the Ga-doped ZnO films are shown in figure 4. The bandgap energy was obtained by extrapolating the linear part of the curves $(\alpha h\nu)^2$ as a function $h\nu$ of the incident radiation to intercept the energy axis (at $\alpha = 0$). The values of energy gap E_g are given in table 1 and are illustrated in figure 4. According to these data,

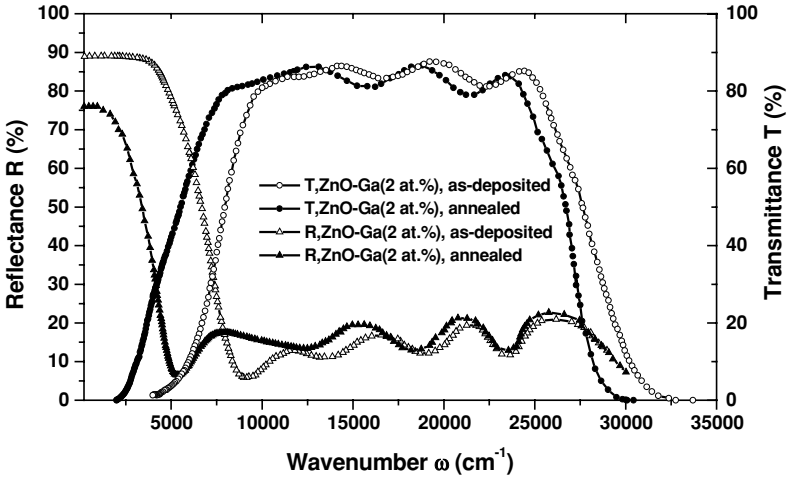

Figure 2. Reflectance and transmittance spectra of the as-deposited and annealed 2 at% Ga-doped ZnO films.

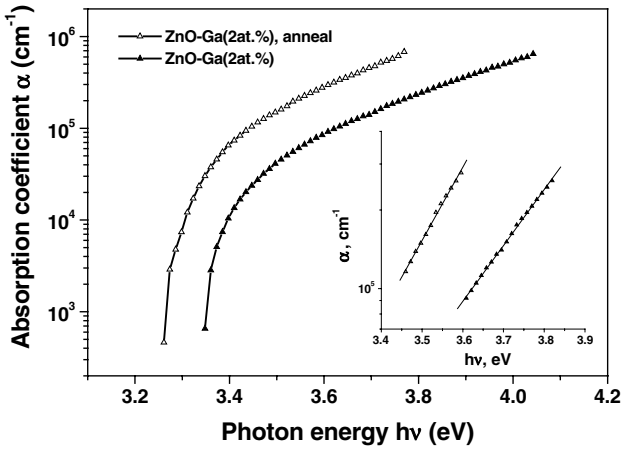

Figure 3. Absorption coefficients near UV edge as a function of $h\nu$ photon energy for the as-deposited and annealed 2 at% Ga-doped ZnO films. The inset shows the linear region of the absorption coefficient, from the slope of which E_0 is calculated.

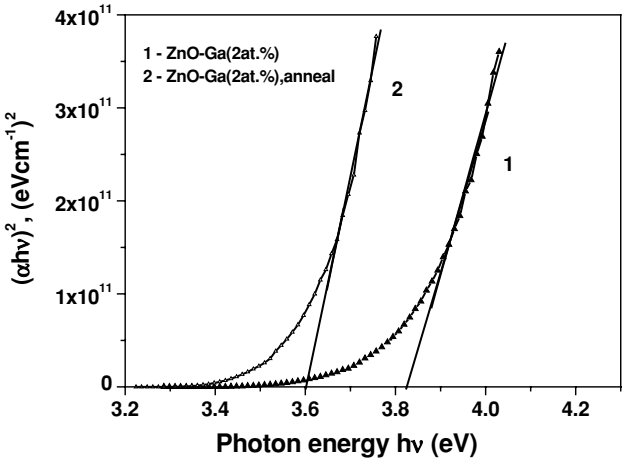

Figure 4. Plots of $(\alpha h\nu)^2$ versus $h\nu$ for the as-deposited and annealed 2 at% Ga-doped ZnO films.

E_g increases from 3.30 to 3.83 eV for both as-deposited pure and as-deposited Ga-doped ZnO films, and from 3.27 to 3.60 eV for the annealed pure and annealed Ga-doped ZnO films. Generally, a blue shift of the absorption edge with an increase of the bandgap is associated with an increase in the carrier concentration (or Burstein–Moss shift) [14, 15]. These results indicate that the Ga atoms work as donors and increase the density of electrons in the conduction band. The donor electrons occupy states at the bottom of the conduction band. Since the Pauli principle prevents doubly occupied states and optical transitions are vertical, the low-energy transitions are blocked.

The energy bandgap widening ΔE_g (the difference in the energy bandgap between Ga-doped and pure ZnO films) is related to the carrier concentration N through the following equation:

$$\Delta E_g = h^2 N^{2/3}/[8m^*(\pi/3)^{2/3}], \tag{1}$$

where h is Planck's constant and m^* is the effective mass of the electron and is approximately equal to 0.35 m_e in ZnO doped with donor atoms. The ΔE_g observed for 2 at% Ga-doped ZnO film gives carrier concentrations of 1.09×10^{21} and 5.3×10^{20} cm^{-3} for the as-deposited and annealed films, respectively. The absorption edge of the heat-treated film in air is shifted towards longer wavelengths in comparison to the as-deposited film. Also, the optical bandgaps of the films significantly decrease after the heat treatment in air, as seen in figure 3.

The absorption coefficient α near the band edge in the energy region of $h\nu < E_g$ empirically follows the exponential law, i.e. the Urbach tail is expressed by

$$\alpha(h\nu) = \alpha_0 \exp(h\nu/E_0). \tag{2}$$

Here α_0 is a constant and E_0 is an empirical parameter, usually weakly dependent on temperature and describing the width of the localized states in the bandgap, but not their energy positions. In [16], E_0 is considered as a parameter that includes the effects of all possible defects. The inset in figure 3 shows the absorption coefficient as a function of photon energy $h\nu$ in a semilogarithmic scale for the ZnO films, where a linear relationship is observed. The slope of the linear fit is used to calculate E_0. The quantities E_0 for the as-deposited and the annealed pure and Ga-doped ZnO films are shown in figure 3 and table 1. The increase of E_0 up to 467 and 356 meV, corresponding to the as-deposited and annealed films, with 2 at% Ga concentration suggests that the atomic structural disorder of the ZnO films increases by Ga doping with respect

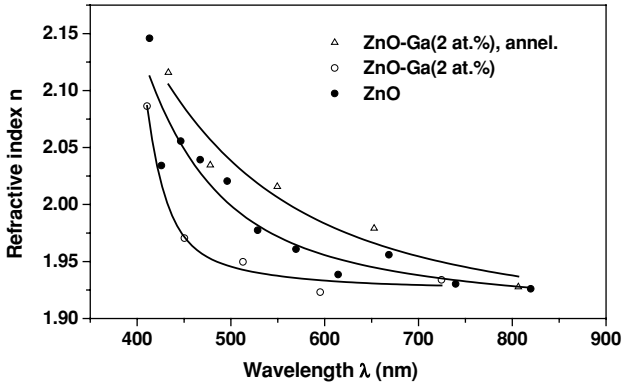

Figure 5. Wavelength dependences of refractive index $n(\lambda)$ for the pure ZnO film and 2 at% Ga-doped as-deposited and annealed ZnO films.

to pure films. The value of E_0 slightly decreases on annealing in air. The optical measurements are correlated with the results of XRD measurements shown in figure 1 and table 1. Thus, it is possible to assume that the stoichiometry between Zn and O can be improved. For the pure ZnO films grown on the sapphire substrates by laser ablation [16], values of E_0 as low as ∼30 meV can be achieved by annealing in air, whereas the as-deposited films show a value >60 meV. The value of E_0 from 80 to 100 meV is given in [17] for the pure ZnO films prepared by the CVD at different formation temperatures. In [18], the values of 70 and 165 meV corresponding to undoped and In-doped ZnO films prepared by the pyrosol process are given.

The refractive index is an important parameter for semiconductor optical device design. In the present work, the refractive index $n(\lambda)$ of the films was evaluated from the interference of the optical transmittance spectra using Swanepoel's envelope method [19]. Figure 5 shows the spectral dependence $n(\lambda)$ for 2 at% as-deposited and annealed Ga-doped ZnO films in the wavelength range from ∼400 to ∼900 nm. For comparison, the refractive index $n(\lambda)$ measured by the same method for pure ZnO film is shown. According to these data, there are significant variations between the refractive index $n(\lambda)$ for the as-deposited Ga-doped ZnO films and the annealed Ga-doped, whereas for the pure as-deposited and annealed in air ZnO films, the variations of the refractive index $n(\lambda)$ are insignificant [9]. In [5], a decrease in refractive index of the Ga-doped ZnO films with respect to pure ZnO films is observed. This difference is explained as due to either a decrease in film density with doping or an increase in the bandgap energy. In our measurements, the increase of bandgap energy for both as-deposited and annealed Ga-doped films with respect to pure film is observed; however, the refractive index for the as-deposited films is higher than for the pure films, while for the annealed ones it is lower.

3.4. Infrared reflectivity measurements

Figure 2 shows reflectivity spectra of 2 at% Ga-doped ZnO films for the as-deposited and annealed samples in the frequency range 30 000–400 cm^{-1}. The spectrum of the as-deposited 2 at% Ga-doped ZnO film is typical for a semiconductor with a high-reflectivity region ($R \sim 90\%$ for $\omega < 5000$ cm^{-1}) due to the screening effect of the free

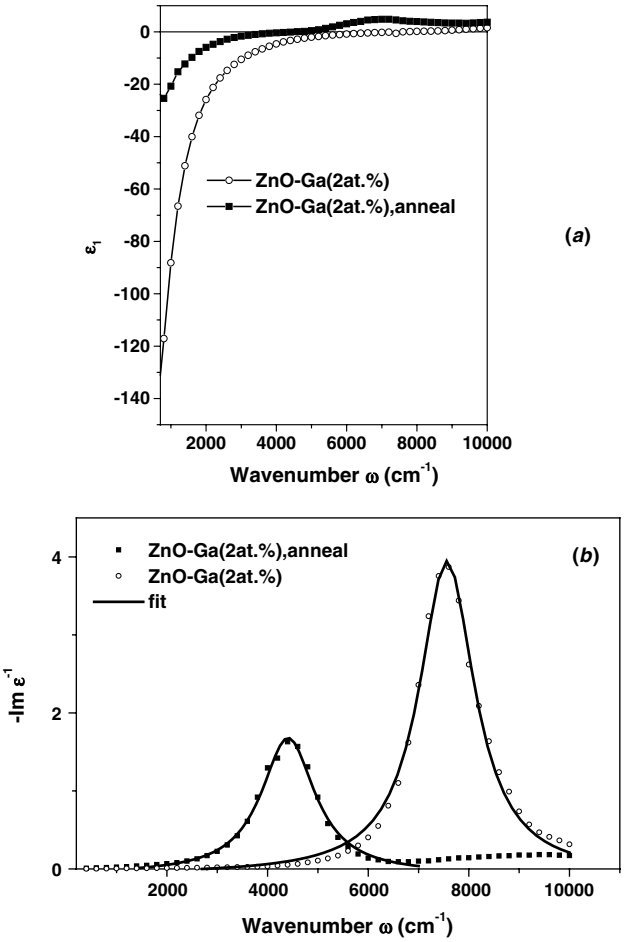

Figure 6. Frequency dependence of (*a*) the real part of the dielectric function, ε_1 and (*b*) loss-energy function, –Im ε^{-1} of the as-deposited and annealed 2 at% Ga-doped ZnO films.

carriers and reflectivity plasma edge near 9000 cm^{-1}. The annealed sample exhibits a plasma shift to lower frequencies (5000 cm^{-1}) and a decrease in reflectivity ($R \sim 75\%$ at $\omega <$ 1000 cm^{-1}). So for frequencies above the plasma edge, the electron plasma is still capable of tuning its oscillation frequency to that of the electromagnetic wave and the material is transparent, whereas below plasma edge the incident light is screened and the material is reflective.

The frequency dependence of optical conductivity, σ, dielectric, ε_1, and energy-loss, –Im ε^{-1}, functions of Ga-doped ZnO films have been calculated by the Kramers–Kronig analysis of the reflectivity spectra and are shown in figures 6 and 7. $\varepsilon_1(\omega)$ is negative at low frequencies, as is appropriate for metals. The energy-loss function, $-\mathrm{Im}\ \varepsilon^{-1}$, in figure 6(*b*) exhibits a significant difference in the position of the loss function maximum for the annealed and as-deposited films. The position of this peak gives the screened plasma frequency, ω_p, and the full width at half-maximum (FWHM) is the value of the scattering rate of the free carriers ($\gamma = 1/\tau$). τ is an effective free-carrier relaxation time that slightly increases in the annealed sample. In table 2, the effective free-carrier relaxation time τ and plasma frequency ω_p of the samples are presented.

All aspects of the relaxation processes are evident in the real part of the optical conductivity shown in figure 7. There

Table 2. Plasma frequency, ω_p, effective free-carrier relaxation time, τ, number of carriers, N/m^* and the Drude resistivity, ρ_{Dr}, of the as-deposited and annealed 2 at% Ga-doped ZnO films.

	ω_p (cm^{-1})	ε_∞	τ (10^{-14} s)	ρ_{Dr} (10^{-3} Ω cm)	μ (cm^2 V^{-1} s^{-1})	N/m^* (10^{21} cm^{-3})
As-deposited	7570	4.0	2.48	0.3	125	2.1
Annealed	4440	4.0	2.56	0.83	128	0.7

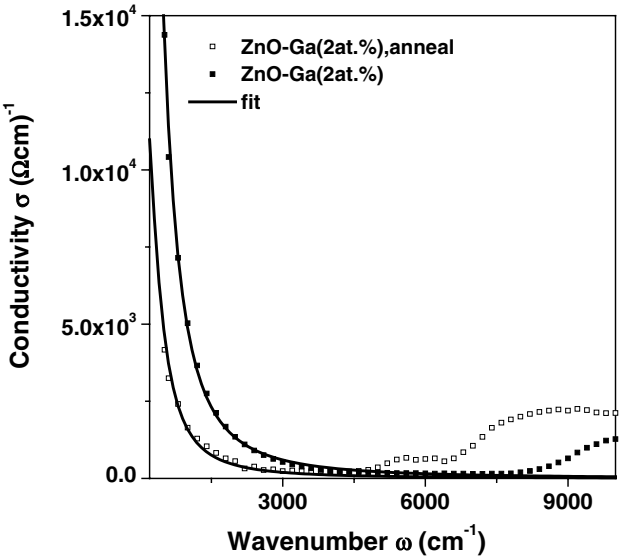

Figure 7. Frequency dependences of the optical conductivity σ for the as-deposited and annealed 2 at% Ga-doped ZnO films. Solid lines are obtained by fitting the Drude model.

is a decrease in the conductivity of the annealed 2 at% Ga-doped ZnO with respect to the as-deposited film. The optical conductivity of 2 at% Ga-doped ZnO may be described by a single Drude model:

$$\sigma(\omega) = \omega_{pD}^2 \gamma_D \big/ 4\pi\left(\omega^2 + \gamma_D^2\right) \tag{3}$$

where ω_{pD} and γ_D are the plasma frequency and free electron damping, respectively.

The solid lines in figure 7 are calculated from the Drude model (3). The excellent fit with the Drude model is achieved for $\omega_{pD} = 7000$ and 4400 cm^{-1} and $\gamma_D = 350$ and 300 cm^{-1} for the as-deposited and annealed samples, respectively. We used the unscreened plasma frequency $\omega_p^2 \varepsilon_\omega = v_p^2$ in fitting. The Drude resistivity obtained from $\rho_{Dr} = 4\pi\gamma \big/ \omega_{pD}^2$ is in satisfactory agreement with the dc electrical resistivity, ρ_{dc}, measured using a standard four-point dc method (see table 2). The slight discrepancy between the optical data and the dc resistivity measurement is related to the estimation of the plasma frequency and relaxation time by optical means.

The plasma of free electrons in ZnO screens the incident electromagnetic wave via intraband transitions within the conduction band with the plasma resonance ω_p given by

$$\omega_p^2 = 4\pi N e^2 / \varepsilon_\infty m^*. \tag{4}$$

where ε_∞ is the contribution from transitions above the highest measured frequency. Since $\varepsilon_\infty = 4.0$, we can estimate $N = 2.1 \times 10^{21}$ cm^{-3} for the as-deposited sample. Annealing at 350 °C for 1 h gives a decrease of the electron concentration to 7.0×10^{20} cm^{-3}, due to the decrease of oxygen vacancies during annealing in air. The scattering rate $\Gamma_p = 1/\tau$ obtained from the energy-loss function –Im ε^{-1} enables us to calculate the optical mobility μ_{opt} in ZnO from the relation $\mu_{opt} = e\tau/m^*$. The obtained values 125 and 128 cm^2 V^{-1} s^{-1} for the as-deposited and annealed samples, respectively, either exceed the carrier mobility data by the Hall measurements ($\mu_{Hall} \sim 68$ cm^2 V^{-1}s^{-1}) as in [3] or are comparable with ones (145 cm^2 V^{-1} s^{-1}) from [20]. According to [21], one might expect that electrons do not cross many grain boundaries because at optical frequencies, the path length for an oscillating electron under the influence of the electromagnetic field is much less than the average grain size in our ZnO of 25 nm. So the contribution of grain boundary scattering in μ_{opt} is insufficient and the optical mobility should be a good indication of the intra-grain values.

4. Conclusions

Transparent conductive films of 2 at% Ga-doped ZnO films have been prepared by e-beam evaporation in vacuum. The crystal structure of the obtained films is hexagonal wurtzite with preferential orientation along the *c*-axis. Doping Ga into the films greatly changes the electrical and optical properties of the films resulting in an increase in the energy bandgap and a decrease in the electrical resistivity due to the increase in carrier concentration. After heat treatment at 350 °C for 1 h in air, it was found that crystallinity and optical quality of the films were improved, but resistivity is slightly increased as a result of the decrease in oxygen vacancies. Absorption and reflectance analysis of the Ga-doped ZnO films has allowed estimation of some conductive characteristics of this material. As a result of independent calculations of carrier concentration from the absorption and reflectance measurements, close values of this parameter were obtained in both cases. The structural, optical and electrical properties of these films make them suitable for transparent electrodes applications in opto-electronic devices and solar cells.

Acknowledgments

The authors would like to thank Shirinyan G for XRD measurements. This work was partially supported by the NFSAT 102-02 grant and Zecotec Innovations Inc (Vancouver, BC, Canada).

References

[1] Miyazaki M, Sato K, Misui A and Nishimura H 1997 *J. Non-Cryst. Solids* **218** 323
[2] Song P K, Watanabe M, Kon M, Mitsui A and Shigesato Y 2002 *Thin Solid Films* **411** 82
[3] Kato H, Sano M, Miyamoto K and Yao T 2002 *J. Cryst. Growth* **237** 538
[4] Yan M, Zhang H T, Widjaja E J and Chang R P H 2003 *J. Appl. Phys.* **94** 5240

[5] Liu Z F, Shan F K, Li Y X, Shin B C and Yu Y S 2003 *J. Cryst. Growth* **259** 130
[6] Cheong K Y, Muti N and Ramanan S R 2002 *Thin Solid Films* **410** 142
[7] Fujihara S, Siziki A and Kimura T 2003 *J. Appl. Phys.* **94** 2411
[8] Ataev B M, Bagamadova A M, Djabrailov A M, Mamedov V V and Rabadanov R A 1995 *Thin Solid Films* **260** 19
[9] Aghamalyan N R, Gambaryan I A, Goulanian E Kh, Hovsepyan R K, Kostanyan R B, Petrosyan S I, Vardanyan E S and Zerrouk A F 2003 *Semicond. Sci. Technol.* **18** 525
[10] Cullity B D 1978 *Elements of X-ray Diffraction* 2nd edn (Reading, MA: Addison-Wesley)
[11] Kreger F A 1964 *The Chemistry of Imperfect Crystals* (Amsterdam: North-Holland) p 650
[12] Hu J and Gordon R G 1992 *J. Appl. Phys.* **72** 5381
[13] Manifacier C, Gasoit J and Fillard J P 1976 *J. Phys. E: Sci. Instrum.* **9** 1002
[14] Burstein E 1954 *Phys. Rev.* **93** 632
[15] Moss T S 1954 *Proc. Phys. Soc. London* B **67** 775
[16] Strikant V and Clarke D R 1997 *J. Appl. Phys.* **81** 6357
[17] Natsume Y, Sakata H, Hirayama T and Yanagita H 1995 *Phys. Status Solidi* a **148** 485
[18] Tokumoto M S, Smith A, Santilli C V, Pulchinelli S H, Craievich A F, Elkaim E, Traverse A and Briois V 2002 *Thin Solid Films* **416** 284
[19] Swanwpoel R 1983 *J. Phys. E: Sci. Instrum.* **16** 1214
[20] Miyamoto K, Sano M, Kato H and Yao T 2004 *J. Cryst. Growth* **265** 34
[21] Joung D L, Coutts T J, Kaydanov V I, Gilmore A S and Mulligan W P 2000 *J. Vac. Sci. Technol.* A **18** 2978